

AdaRing: Towards Ultra-Light Vision-Language Adaptation via Cross-Layer Tensor Ring Decomposition

Ying Huang¹, Yuanbin Man¹, Wenqi Jia¹, Zhengzhong Tu², Junzhou Huang¹, Miao Yin^{1†}

¹University of Texas at Arlington, ²Texas A&M University

{ying.huang, yuanbin.man, wenqi.jia}@uta.edu, tzz@tamu.edu,

{jzhuang, miao.yin}@uta.edu

Abstract

Adapter-based fine-tuning has gained remarkable attention in adapting large pre-trained vision language models (VLMs) for a wide range of downstream tasks efficiently. In this paradigm, only the inserted adapters are fine-tuned, without the need for training the original VLM backbone. Existing works scale adapters by integrating them into every layer of VLMs to increase the capacity of adapters. However, these methods face two primary limitations: 1) limited compression rate due to ignoring cross-layer redundancy, and 2) limited representational capacity across homogeneous adapters. In this paper, we propose a novel vision-language fine-tuning framework based on cross-layer tensor ring decomposition (TRD) with the integration and collaboration of diverse adapters, called AdaRing, achieving ultra-light parameter-efficient adaptation of VLMs on various tasks. To remove the high redundancy that exists among adapters across layers, we exploit the tensor-level low-rankness to formulate adapters as layer-shared tensor cores and layer-specific slices. Moreover, guided by generalization-aware fine-tuning, diverse rank-driven adapters cooperate to handle tasks that require different representations. Our experiments show that the proposed AdaRing achieves the state-of-the-art performance while reducing average training parameters by 90%.

1. Introduction

Vision-Language Models (VLMs) adaptation [5, 19, 48, 49] has gained substantial attention in the fields of computer vision (CV) and natural language processing (NLP), as a means of adapting VLMs, e.g., CLIP [17] and ALIGN [30], pre-trained from web-scale image-text pairs into multiple downstream tasks. Despite the effectiveness of representations that benefit from large-scale pre-training, fine-tuning VLMs for downstream tasks still faces several challenges,

[†]Corresponding author.

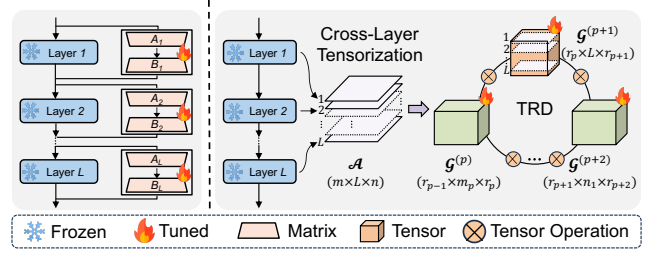


Figure 1. (Left) Existing methods utilize regular matrix decomposition layer by layer, leading to significant redundancy and limited representation capability. (Right) Our **AdaRing** achieves ultra-light adaptation via cross-layer tensor ring decomposition (TRD).

especially the challenge of *massive fine-tuning parameters*, which results in heavy computational costs and a significant memory burden [18, 28, 35].

Adapter-based fine-tuning [10, 47] is the mainstream paradigm to mitigate this issue, where small trainable adapters, typically implemented as two linear layers, are inserted into the final layer of the VLM. During training, only these lightweight modules are fine-tuned, while the rest of the parameters in the VLM backbone remain frozen. This approach drastically reduces the number of trainable parameters. However, confining the adaptation to only the final layer severely limits the model’s capacity to capture the complex information required by real-world vision-language tasks.

To address this limitation, existing methods scale adapters beyond the final layer, either *vertically*, by inserting them into every transformer block [3, 40], or *horizontally*, by introducing multiple adapters within a single block [45]. While these schemes improve performance, they still face two main limitations. 1) Inadequate compression rate. Based on the hypothesis that the adapter weight has a low “intrinsic rank”, current methods leverage *low-rank matrix decomposition* [15] for every adapter independently to reduce training parameters in Figure 1. However, such matrix-level decomposition methods still

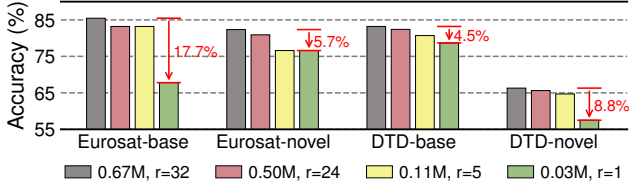


Figure 2. Matrix decomposition-based approaches (e.g., MMA) suffer from rapid performance degradation as the number of trainable parameters decreases on the DTD and EuroSAT datasets.

have a significant accuracy decrease with insufficient compression rates as shown in Figure 2. Moreover, these approaches ignore the redundancy across adapters of different layers, resulting in a large number of training parameters, especially in the large VLM with deep layers. 2) Limited representational capacity across homogeneous adapters. Most existing methods introduce multiple uniform, homogeneous adapters within a single layer, which tend to learn similar features during fine-tuning. This lack of diversity makes it challenging to meet the varied demands of different features for tasks, hindering the model’s ability to generalize across varied tasks [33]. *Quantitative analysis* is presented in the following Section 4.

To address those limitations, we propose, AdaRing, an ultra-light vision-language adaptation framework using cross-layer tensor ring decomposition. Specifically, instead of applying low-rank approximation to each layer’s weight matrix independently, we consider stacking the adapters across layers into a higher-order tensor, and then compressing it to reduce both intra-layer and cross-layer redundancy. Fortunately, *tensor decomposition* [38, 44] offers a principled way to achieve this: it decomposes the original large, high-dimensional weight tensor into a sequence of compact tensor cores, leading to a significant reduction in training parameters. Moreover, the rank of each tensor core provides a mechanism to modulate the model’s representational specializations [33, 37]. Motivated by these advantages, we conduct an in-depth exploration of tensor decomposition-based VLM adaptation with diverse adapters. First, we investigate the redundancy of cross-layer adapters, which opens opportunities for achieving an ultra-light adapter based on cross-layer tensor decomposition. Second, we explore different variants of tensor decomposition, showing that the adapter of tensor ring [46] format has more powerful and separate representation abilities than other format, as observed in our experiments with CLIP. Third, to design adapters that can handle various downstream tasks effectively, we equip CLIP with diverse adapters and achieve better performance than homogeneous adapters.

Building on these insights, we propose AdaRing, a novel fine-tuning framework based on cross-layer tensor ring (TR) decomposition with the integration and collabora-

tion of diverse adapters, to achieve extremely parameter-efficient adaptation of VLMs for varied tasks. Our key contribution can be summarized as follows:

- We creatively reduce the cross-layer redundancy by exploiting the tensor-level low-rankness, stacking all adapters across different layers, and decomposing it into a high-dimensional tensor with layer-shared and layer-specific cores. Our framework achieves ultra-light adaptation on real-world tasks.
- We equip VLMs with diverse adapters guided by rank to handle varied tasks, and a learnable combinator is then designed to coordinate their collaboration adaptively. We propose generalization-aware fine-tuning to improve performance on previously unseen data.
- We conduct experiments on extensive downstream fine-tuning tasks. Our AdaRing achieves the best average performance over 11 datasets and outperforms the previous state-of-the-art MMA [40] under almost all few-shot scenarios in the OxfordFlowers dataset. Moreover, AdaRing reduces the average training parameters by 90%, highlighting superior performance and efficiency in practice.

2. Related Work

Parameter-efficient Fine-tuning. Parameter-efficient fine-tuning technique aims to transfer pretrained models, e.g., CLIP [17], to downstream tasks by only fine-tuning a few trainable parameters for efficiency [4, 24, 29]. In general, it can be realized via either prompt tuning, adapter tuning, or reparameterization tuning. **Prompt tuning** involves incorporating handcrafted or learnable prompts to facilitate the fine-tuning of a pre-trained model [43, 48, 49]. PromptKD leverages a two-stage prompt tuning process to encourage the knowledge distillation from a large teacher model to a lightweight target model [23]. Instead of fine-tuning input prompts, **adapter tuning** proposes to insert some small modules into the original model, and only these inserted modules are optimized during fine-tuning [10]. Existing adapter tuning methods are mainly built upon *layer-wise* adapters [47]. For example, MMA [40] adds the new adapter into higher layers of models to provide alignment between vision-language representations. In addition, [45] introduces MoE structure onto each layer of frozen CLIP, enabling the dynamic expansion of a pre-trained CLIP model. However, these methods ignore the parameter redundancy among adapters of different layers, leading to a substantial increase in computational burden as model layers increase.

Low-rank Matrix & Tensor Decomposition of Weight Matrices. Low-rank decomposition is a powerful compression tool that can reduce model size and bring considerable speedup. It can broadly be categorized into matrix decomposition and tensor decomposition. **Matrix decomposition** factorizes the large weight matrix into small matrix com-

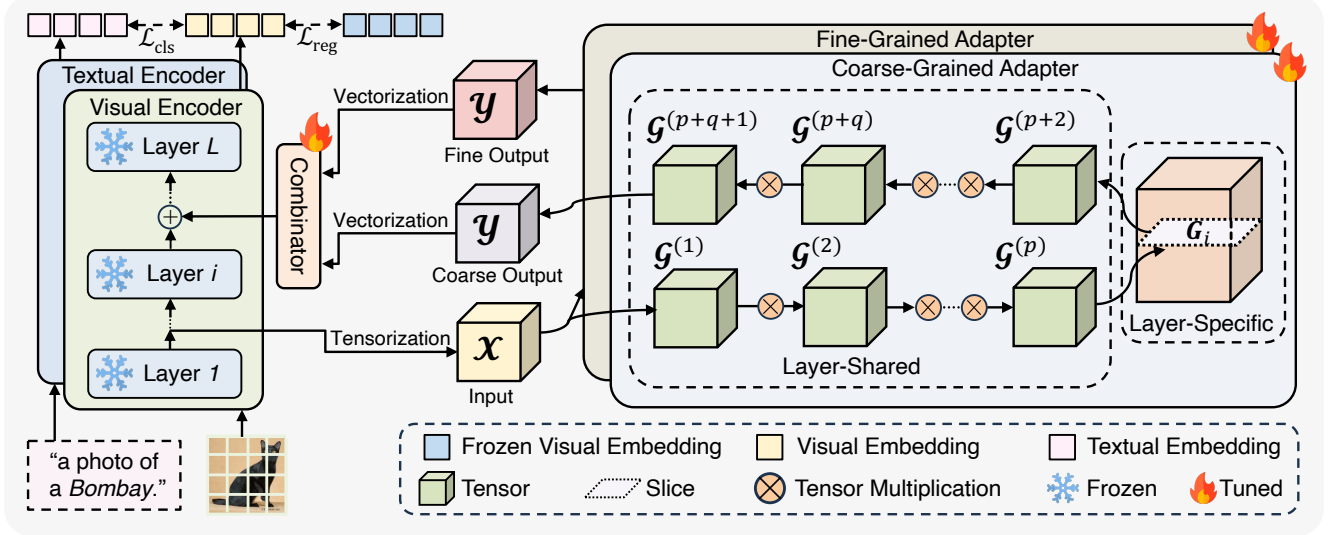


Figure 3. The framework of AdaRing. With image and text as inputs, AdaRing equips the i -th encoder layer with fine-grained adapter and coarse-grained adapter to handle tasks that require distinct representational capacities. The adapter consists of the layer-shared tensor cores and the layer-specific slice to extract redundancy across adapters and simultaneously preserve layer-specific information. During fine-tuning, the textual and visual encoders remain entirely frozen, while the adapter is trained to minimize cross-entropy loss \mathcal{L}_{cls} combined with a generalization-aware regularization term \mathcal{L}_{reg} , retaining strong discrimination while enhancing generalization in downstream tasks.

ponents [12, 13, 16]. However, these approaches do not fully exploit the inherent spatial low-rankness of the weight, causing significant accuracy loss with limited compression ratios. To address these limitations, **tensor decomposition**, such as Tucker [32] and Tensor Train [11, 41, 42], factorizes the original high-order tensor in the high-dimensional space [34], which can bring impressive compression performance. In this paper, we efficiently tensorize and decompose the weight matrices of the adapters during fine-tuning VLMs. Moreover, instead of applying tensor decomposition to each layer-wise adapter independently, we utilize *cross-layer* tensor decomposition to simultaneously reduce inter-layer and intra-layer redundancy.

3. Background

3.1. Notation

Throughout this paper, vectors, matrices, and tensors are denoted by bold lowercase letters, bold uppercase letters, and bold calligraphic letters, respectively, e.g., \mathbf{a} , \mathbf{A} and \mathcal{A} . Also, $\mathcal{A}_{(i_1, \dots, i_d)}$ denotes the single entry of d -order tensor \mathcal{A} .

3.2. Adapter Tuning Basics

Adapter tuning achieves comparable performance to fine-tuning VLM (CLIP [8, 17] in this work) for many downstream tasks by keeping the backbone visual encoder \mathcal{V} and textual encoder \mathcal{T} frozen and only fine-tuning additional inserted visual adapter and textual adapter.

Recent works insert adapters into each layer to increase the capacities, thereby improving fine-tuning performance. Moreover, in order to alleviate the training costs caused by substantial fine-tuning parameters, they use two sequential low-rank matrices $\mathbf{A}_l \in \mathbb{R}^{I \times r}$ and $\mathbf{B}_l \in \mathbb{R}^{r \times O}$ as each layer-wise adapter \mathcal{F}_l [15]. The forward computation for the l -th layer is written as:

$$\begin{aligned} \mathbf{y}^v &= \mathcal{V}_l(\mathbf{x}^v) + \alpha \mathbf{A}_l^v \mathbf{B}_l^v \mathbf{x}^v, \\ \mathbf{y}^t &= \mathcal{T}_l(\mathbf{x}^t) + \beta \mathbf{A}_l^t \mathbf{B}_l^t \mathbf{x}^t, \end{aligned} \quad (1)$$

where \mathcal{V}_l , \mathbf{x}^v and \mathbf{y}^v denote the l -th visual encoder layer, corresponding input and output visual embeddings, respectively; \mathcal{T}_l , \mathbf{x}^t and \mathbf{y}^t represent the l -th textual encoder layer, corresponding input and output textual embeddings, respectively; α and β are coefficients to merge embeddings produced by the frozen encoder layer and adapter. Finally, the specific image feature f^v and text feature f^t are obtained from the last layer. The adapters are trained to maximize the similarity of f^v and the corresponding f^t .

3.3. Tensor Ring Decomposition Basics

Given a d -order tensor $\mathcal{A} \in \mathbb{R}^{n_1 \times n_2 \times \dots \times n_d}$, tensor ring decomposition (TRD) [46] can represent it with a sequence of 3-order core tensors $\mathcal{G}^j \in \mathbb{R}^{R_{j-1} \times n_j \times R_j}$ as follows:

$$\begin{aligned} \mathcal{A}_{(i_1, i_2, \dots, i_d)} &= \sum_{r_0=r_d, r_1, \dots, r_{d-1}}^{R_0, R_1, \dots, R_{d-1}} \mathcal{G}_{(r_0, i_1, r_1)}^1 \mathcal{G}_{(r_1, i_2, r_2)}^2 \dots \mathcal{G}_{(r_{d-1}, i_d, r_d)}^d, \end{aligned} \quad (2)$$

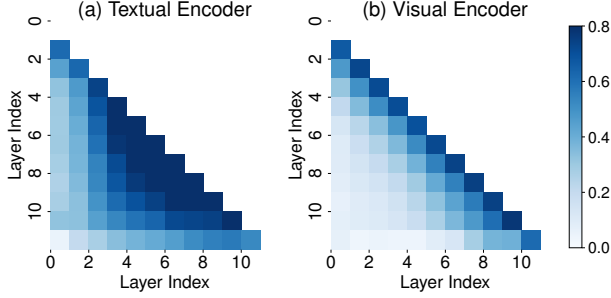


Figure 4. Cosine similarity of embeddings between layers (a) textual encoder (b) visual encoder.

where R_0, R_1, \dots, R_d are called ranks and $R_0 = R_d$. By treating the latent cores equivalently and capturing complex dependencies, TRD enables compact and flexible representation of high-dimensional data [39].

4. Motivation

In this section, we present the motivation for our proposed ultra-light parameter-efficient VLM adaptation on various downstream tasks. We first investigate the redundancy across adapters, which motivates us to construct an ultra-light adapter based on cross-layer tensor decomposition. Then, we compare the representation abilities of adapters achieved by different tensor decomposition strategies. Finally, we analyze how the rank of the adapter affects the fine-tuning performance based on the chosen tensor decomposition method.

Observation 1: *High redundancy exists among adapters across all layers.* In Figure 4, we display the similarities between the embeddings of each layer using data from the OxfordPets dataset [27]. The dark color represents high similarities between the embeddings from two different layers. We can observe that cosine similarity exceeds 80% between two adjacent embeddings. Moreover, a high correlation persists even across layers with large intervals, suggesting that it’s parameter-inefficient to employ the layer-level adapters. To mitigate this redundancy, we propose to exploit the tensor-level low-rankness along the layer dimension by performing tensor decomposition, leading to the following observations.

Observation 2: *Adapter with tensor ring structure has more powerful and separate representation abilities, compared to other tensor decomposition methods.* To select an optimal tensor decomposition strategy that achieves both high compression rate and strong representational abilities, we conduct fine-tuning on the DTD dataset using an adapter achieved by tensor ring decomposition (TRD) [46] and tensor train decomposition (TTD) [41], respectively. In Figure 5, we visualize the cosine similarity of textual embeddings for 47 classes. Lighter colors indicate lower simi-

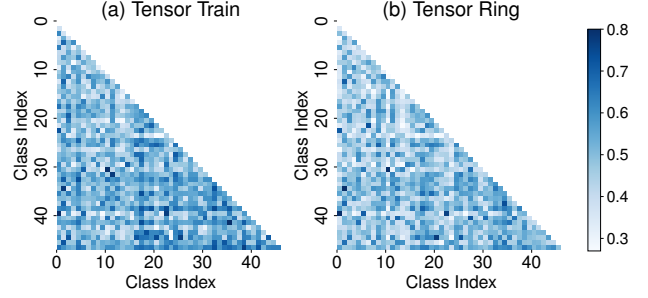


Figure 5. Cosine similarity of textual embeddings with (a) Tensor Train decomposition and (b) Tensor Ring decomposition.

larity. This visualization shows that textual embeddings of different classes produced by the TR adapter exhibit less similarity and greater separation in the feature space, which can reduce the misclassification risk. We reason that better separability is gained by removing the constraints over ranks and treating the latent cores equivalently within the TRD process, thereby offering more freedom in finding the optimal representations. However, TTD highly depends on permutations of tensor cores, leading to difficulties in finding the optimal representations [46]. Correspondingly, we propose to utilize TRD to achieve an ultra-compact adapter by decomposing the original cross-layer stacked adapters.

Observation 3: *Adapters with different ranks exhibit different expertise.* To design adapters that can handle various downstream tasks effectively, we explore two tasks following previous works [2, 48]: 1) base task—testing on seen data; 2) novel task—testing on unseen data. These tasks emphasize different capabilities: discrimination for the base task and generalization for the novel task. Figure 6 (a) shows that CLIP with the large-rank adapter performs better on the base task, reflecting stronger discrimination, while CLIP with the small-rank adapter is more generalizable to the novel task. Additionally, compared to the one with a large-rank adapter in Figure 6 (b), CLIP with a small-rank adapter generates visual embeddings that are more similar to those of the frozen CLIP, while the frozen CLIP is proven to have strong generalization abilities that benefited from large-scale pretraining. We posit that this divergence is an artifact of parameter count: the large-rank adapter with more parameters is inclined toward capturing discriminative information, while the small-rank adapter with fewer parameters is prone to preserving the generalization ability of a pre-trained model. The distinct expertise between adapters offers valuable insights for enhancing both discrimination and generalization, suggesting that adapters of varied ranks can cooperate to handle inputs that require distinct representational capacities.

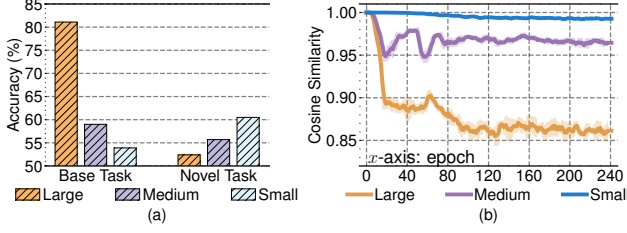


Figure 6. Analysis of diverse adapters. (a) The accuracy in the base and novel tasks. (b) The similarity between the visual embeddings from the frozen CLIP and those from CLIP with fine-tuned adapters.

5. Methodology: AdaRing

In this section, we introduce the proposed AdaRing, an ultra-light parameter-efficient VLM adaptation framework. We first introduce the cross-layer tensor ring decomposition to address the parameter redundancy among layer-wise adapters in Section 5.1. Then, we delineate the collaboration of rank-driven adapters for handling various downstream tasks in Section 5.2. Finally, we propose the generalization-aware fine-tuning to further encourage rank-driven adapters to cooperate efficiently in Section 5.3.

5.1. Adaptation with Cross-Layer Tensor Ring Decomposition

Observation 1 reveals redundancy among layer-wise adapters, while Observation 2 demonstrates that adapters with tensor ring (TR) structure have more powerful and separate representation capabilities. Therefore, we propose to design cross-layer adapters with the TR structure to reduce fine-tuning parameters, which involves *Cross-Layer Tensorization* and *Ring-based Decomposition*. Finally, the *TR-Structure Adapter* is fine-tuned towards downstream tasks.

Cross-Layer Tensorization. *Tensorization* is used to transform a 2-D weight matrix into a high-dimensional tensor. Considering the redundancy among layer-wise adapters, we employ *Cross-Layer Tensorization* for their weight matrices to facilitate low-rankness exploration across layer dimension. Specifically, L adapter weights can be collected and stacked as $\{\mathbf{A}_i \in \mathbb{R}^{I \times O}\}_{i=1}^L$ and then reshaped as $\mathcal{A} \in \mathbb{R}^{I_1 \times \dots \times I_p \times L \times O_1 \times \dots \times O_q}$, where $I = \prod_{j=1}^p I_j$ and $O = \prod_{j=1}^q O_j$.

Ring-based Decomposition. After tensorizing these adapters into a high-dimensional tensor \mathcal{A} , it can be then decomposed into the TR format with $p + q + 1$ core tensors \mathcal{G}^j multiplied one by one, each of which corresponds to an input dimension, layer dimension or an output dimension, referring to Eq. 2. The element of tensor \mathcal{A} is explicitly

calculated as:

$$\mathcal{A}_{(i_1, \dots, i_p, l, o_1, \dots, o_q)} = \sum_{r_0, \dots, r_{p+q}} \mathcal{G}_{(r_0, i_1, r_1)}^1 \cdots \mathcal{G}_{(r_{p-1}, i_p, r_p)}^p \mathcal{G}_{(r_p, l, r_{p+1})}^{p+1} \mathcal{G}_{(r_{p+1}, o_1, r_{p+2})}^{p+2} \cdots \mathcal{G}_{(r_{p+q}, o_q, r_0)}^{p+q+1}. \quad (3)$$

In particular, $\mathcal{G}^{p+1} \in \mathbb{R}^{R_p \times L \times R_{p+1}}$ is the decomposed component along layer dimension, with the layer rank parameter $R_p(R_{p+1})$ controlling the low-rankness of stacked adapter weight matrices.

Analysis of training parameters. By exploiting the low-rank property of adapter weights, AdaRing adds only $R_{p+1}R_{p+2}L + \sum_{j=1}^p R_j R_{j+1} I_j + \sum_{j=p+2}^{p+q+1} R_j R_{j+1} O_j$ parameters. Since R_{p+1} and R_{p+2} are small values, it alleviates the parameter-efficiency dilemma for the large model with deep layers and wide dimensions. In contrast, existing methods ignore the redundancy across adapters, causing the number of training parameters $(I + O) * r * L$ to increase drastically with the increase of layers.

TR-Structure Adapter. Based on *Cross-Layer Tensorization* and *Ring-based Decomposition*, AdaRing explicitly determines the structural form of the adapter, referred to as the TR-Structure adapter. It should be noted that the adapter remains in its low-rank tensor format throughout fine-tuning, meaning it is trained to decompose. AdaRing extracts and formulates the redundant components as layer-shared tensor cores. As a result, the layer-wise components can be made substantially smaller, while still retaining the layer-specific characteristics. Specifically, $\{\mathcal{G}^1, \dots, \mathcal{G}^p, \mathcal{G}^{p+2}, \dots, \mathcal{G}^{p+q+1}\}$ are shared tensor cores among layers to capture the layer-shared information, while the slice $G_l = \mathcal{G}_{(:, l, :)}^{p+1} \in \mathbb{R}^{R_p \times R_{p+1}}$ is specific to the adapter \mathcal{F}_l at the l -th layer.

We use different initialization strategies for different components of the adapter. Specifically, the layer-specific slice G_l is initialized to zeros to make the initial model’s behavior match that of the original CLIP. Layer-shared tensor cores are initialized from the Gaussian distribution, encouraging the optimizer to explore diverse update directions [42].

The forward computation within the adapter \mathcal{F}_l at the l -th layer from input embedding \mathbf{x} to output embedding \mathbf{y} is defined as:

$$\mathbf{y} = \mathcal{F}_l(\mathbf{x}). \quad (4)$$

It involves the process of “*Tensorization-Tensor Multiplication-Vectorization*”:

1 *Tensorization.* The input embedding of the l -th layer $\mathbf{x} \in \mathbb{R}^I$ is first tensorized into the high-dimensional tensor $\mathcal{X} \in \mathbb{R}^{I_1 \times \dots \times I_p}$.

2 *Tensor Multiplication.* The input tensor $\mathcal{X} \in \mathbb{R}^{I_1 \times \dots \times I_p}$ then multiplies with layer-shared tensor cores

and layer-specific slice sequentially:

$$\mathcal{Y}_{(o_1, \dots, o_q)} = \sum_{i_1, \dots, i_p} \sum_{r_0, \dots, r_{p+q}} \mathcal{X}_{(i_1, \dots, i_p)} \mathcal{G}_{(r_0, i_1, r_1)}^1 \cdots \mathcal{G}_{(r_{p-1}, i_p, r_p)}^p G_l \mathcal{G}_{(r_{p+1}, o_1, r_{p+2})}^{p+2} \cdots \mathcal{G}_{(r_{p+q}, o_d, r_0)}^{p+q+1}. \quad (5)$$

3 Vectorization. Given that the desired output \mathbf{y} of the adapter is a vector, the output tensor $\mathcal{Y} \in \mathbb{R}^{O_1 \times \dots \times O_q}$ is finally reshaped into 1-D format $\mathbf{y} \in \mathbb{R}^O$, where $O = \prod_{j=1}^q O_j$.

5.2. Collaboration of Rank-Driven Adapters

The selection of layer rank directly affects the capacity of the layer and the number of training parameters. Observation 3 shows that adapters with different ranks have different expertise across tasks. Therefore, AdaRing designs the collaboration of *fine-grained adapter* with relatively large rank and *coarse-grained adapter* with extremely small rank to capture discriminative and generalizable knowledge simultaneously. The overall forward process at the l -th layer is expressed as:

$$\begin{aligned} \mathbf{y}^v &= \mathcal{V}_l(\mathbf{x}^v) + \bar{\alpha} \bar{\mathcal{F}}_l^v(\mathbf{x}^v) + \hat{\alpha} \hat{\mathcal{F}}_l^v(\mathbf{x}^v), \\ \mathbf{y}^t &= \mathcal{T}_l(\mathbf{x}^t) + \bar{\beta} \bar{\mathcal{F}}_l^t(\mathbf{x}^t) + \hat{\beta} \hat{\mathcal{F}}_l^t(\mathbf{x}^t), \end{aligned} \quad (6)$$

where $\bar{\mathcal{F}}_l^v$ and $\hat{\mathcal{F}}_l^v$ are fine-grained and coarse-grained adapters for visual encoder, respectively. The fused weights $\bar{\alpha}$ and $\hat{\alpha}$ are generated by a combinator composed of a single learnable linear layer, enabling the collaboration between adapters in a data-adaptive manner. The adaptive collaboration is also applied to the textual encoder.

5.3. Generalization-Aware Fine-Tuning

To further encourage diverse rank-driven adapters to cooperate towards downstream tasks, we propose the generalization-aware fine-tuning, thereby fully leveraging the different expertise of diverse rank-driven adapters. Specifically, during fine-tuning, given an image I with the corresponding text prompt “a photo of a $\{y\}$ ”, the backbone encoders \mathcal{V} and \mathcal{T} are frozen, while the weights of adapters are learned to maximize cosine similarity between output visual embedding f^v and text embedding f^t following the cross-entropy loss:

$$\mathcal{L}_{\text{cls}} = - \sum_{I \in \mathcal{I}} \log \frac{\exp(\cos(f^v, f_y^t)/\tau)}{\sum_{c=1}^C \exp(\cos(f^v, f_c^t)/\tau)}, \quad (7)$$

where C is the number of classes and τ is the temperature.

The cross-entropy loss \mathcal{L}_{cls} encourages the model to focus on discriminative information from seen data (base task), leading the combinator to favor the fine-grained adapter. However, since unseen data (novel task) is unavailable during training, the model lacks guidance to generalize

well, resulting in the coarse-grained adapter being underutilized. To address this, we propose a generalization-aware regularization term that proactively encourages the coarse-grained adapter to participate during training. Specifically, this term minimizes the distance between fine-tuned and frozen CLIP embeddings.

$$\mathcal{L}_{\text{reg}} = \sum_{I \in \mathcal{I}} (1 - \cos(f^v, \mathcal{V}(I))). \quad (8)$$

The overall training loss is $\mathcal{L} = \mathcal{L}_{\text{cls}} + \lambda \mathcal{L}_{\text{reg}}$, where λ is the preservation ratio. By considering these two terms, AdaRing retains strong discrimination while enhancing generalization on tasks.

6. Experiments

Datasets. Following [40], we conduct experiments on 11 image classification datasets, i.e., ImageNet [7] and Caltech [9] for generic object classification; OxfordPets [27], StanfordCars [21], OxfordFlowers [26], Food101 [1], and FGVC Aircraft [25] for fine-grained visual categorization, EuroSAT [14] for satellite image classification, UCF101 [31] for action recognition, DTD [6] for texture classification, and SUN397 [36] for scene understanding.

Baselines. On all datasets, we compare our proposed AdaRing with zero-shot CLIP [30], prompt tuning approaches including CoOp [49], KgCoOp [43], MaPLe [20], LASP [2], RPO [22], PromptKD [23] and existing state-of-the-art adapter-based fine-tuning approaches, BSLoRA [50], MMA [40].

Implementation Details. Following previous works, we conduct experiments with the few-shot setting, i.e. 16 shots per category. We use ViT-B/16 based CLIP model in all settings of experiments and train our models for 10 epochs. On the large-scale ImageNet dataset, we use a batch size of 128 for training. On the other 10 datasets, we set the batch size to 16.

6.1. Main Results

We compare AdaRing with state-of-the-art methods on the 11 widely used datasets of base and novel tasks, as well as harmonic mean (HM) of accuracies on base and novel tasks. As illustrated in Table 1, our AdaRing demonstrates superior average performance across 11 datasets, ranking first on base and novel tasks in 9 of them. Notably, on the EuroSAT dataset, AdaRing attains 95.04% on the base task and 85.87% on the novel task, outperforming MMA, the adapter tuning-based approach with the second-best average performance, by 12.21% and 3.53%, respectively. Moreover, Bi-Share (GT) exhibits a significant performance drop on the fine-grained dataset FGVC Aircraft. We argue that it’s because the lossy process of one-rank decomposition to gates hinders the model from capturing fine-grained information. These results show that our approach achieves

Table 1. Comparison with state-of-the-art methods on the 11 datasets. “Base” and “Novel” are the recognition accuracies on base and novel tasks, respectively. “HM” is the harmonic mean of these two accuracies.

	Method	Average			Caltech101			OxfordPets			ImageNet		
		Base	Novel	HM	Base	Novel	HM	Base	Novel	HM	Base	Novel	HM
<i>Zero-shot Inference</i>	CLIP	69.34	74.22	71.70	96.84	94.00	95.40	91.17	97.26	94.12	72.43	64.18	70.22
<i>Prompt Tuning</i>	CoOp	82.69	65.23	72.66	98.00	89.13	93.67	95.26	94.47	94.87	74.67	67.88	71.92
	KgCoOp	80.73	73.60	77.03	97.72	94.39	96.03	94.65	97.76	96.18	75.83	69.26	72.78
	MaPLe	82.28	75.14	78.55	97.74	94.36	96.02	95.43	97.76	96.58	76.66	70.54	73.47
	LASP	82.70	74.90	78.61	98.10	94.24	96.16	95.90	97.93	96.90	76.20	70.95	73.48
	RPO	81.13	75.00	77.78	97.97	94.37	96.03	94.63	97.50	96.05	76.60	71.57	74.00
	PromptKD	86.96	80.73	83.73	98.91	96.65	97.77	96.30	98.01	97.15	80.83	74.66	77.62
<i>Adapter Tuning</i>	BSLoRA (SS)	82.84	74.06	78.20	98.51	94.54	96.48	94.94	97.87	96.38	77.40	70.44	73.75
	BSLoRA (GT)	82.79	73.91	78.09	97.80	94.97	96.36	95.85	97.25	96.54	77.48	70.20	73.66
	MMA	83.20	76.80	79.87	98.40	94.00	96.15	95.40	98.07	96.72	77.31	71.00	74.02
	AdaRing	87.16	81.12	84.03	99.00	96.84	97.91	96.46	98.31	97.38	80.07	73.97	76.90
	Method	UCF101			EuroSAT			FGVCAircraft			Food101		
		Base	Novel	HM	Base	Novel	HM	Base	Novel	HM	Base	Novel	HM
<i>Zero-shot Inference</i>	CLIP	70.53	77.50	73.85	56.48	64.05	60.03	27.19	36.29	31.09	90.10	91.22	90.66
<i>Prompt Tuning</i>	CoOp	84.69	56.05	67.46	92.19	54.74	68.69	40.44	22.30	28.75	88.33	82.26	85.19
	KgCoOp	82.89	76.67	79.65	85.64	64.34	73.48	36.21	33.55	34.83	90.50	91.70	91.09
	MaPLe	83.00	78.66	80.77	94.07	73.23	82.35	37.44	35.61	36.50	90.71	92.05	91.38
	LASP	84.77	78.03	81.26	94.60	77.78	85.36	34.53	30.57	32.43	91.20	91.70	91.44
	RPO	83.67	75.43	79.34	86.63	68.97	76.79	37.33	34.20	35.70	90.33	90.83	90.58
	PromptKD	89.71	82.27	86.10	97.54	82.08	89.14	49.12	41.81	45.17	92.43	93.68	93.05
<i>Adapter Tuning</i>	BSLoRA (SS)	85.47	79.07	82.14	83.74	76.59	80.00	42.25	29.99	35.08	89.70	90.44	90.07
	BSLoRA (GT)	85.88	76.42	80.87	83.59	77.87	80.63	39.61	27.41	32.40	89.01	90.68	89.84
	MMA	86.23	80.03	82.20	85.46	82.34	83.87	40.57	36.33	38.33	90.13	91.30	90.71
	AdaRing	89.93	82.64	86.13	97.67	85.87	91.39	49.37	41.98	45.38	93.53	94.02	93.77
	Method	SUN397			DTD			StanfordCars			OxfordFlowers		
		Base	Novel	HM	Base	Novel	HM	Base	Novel	HM	Base	Novel	HM
<i>Zero-shot Inference</i>	CLIP	69.36	75.35	72.23	53.24	59.90	56.37	63.37	74.89	68.65	72.08	77.80	74.83
<i>Prompt Tuning</i>	CoOp	80.60	65.89	72.51	79.44	41.18	54.24	78.12	60.40	68.13	97.60	59.67	74.06
	KgCoOp	80.29	76.53	78.36	77.55	54.99	64.35	71.76	75.04	73.36	95.00	74.73	83.65
	MaPLe	80.82	78.70	79.75	80.36	59.18	68.16	72.94	74.00	73.47	95.92	72.46	82.56
	LASP	80.70	78.60	79.63	81.40	58.60	68.14	75.17	71.60	73.34	97.00	73.53	83.95
	RPO	80.60	77.80	79.18	76.70	62.13	68.61	73.87	75.53	74.69	94.13	76.67	84.50
	PromptKD	83.69	81.54	82.60	85.84	71.37	77.94	82.80	83.37	83.13	99.42	82.62	90.24
<i>Adapter Tuning</i>	BSLoRA (SS)	81.75	75.88	78.70	82.52	58.45	68.43	77.64	74.58	76.08	97.34	66.80	79.23
	BSLoRA (GT)	81.84	75.84	78.73	83.21	56.15	67.05	79.03	74.44	76.66	97.34	71.77	82.62
	MMA	82.27	78.57	80.38	83.20	65.63	73.38	78.50	73.10	75.70	97.77	75.93	85.48
	AdaRing	83.72	81.99	82.85	86.04	72.39	78.63	83.47	84.05	83.76	99.51	80.25	88.85

both discriminative and generalizable performance in varied downstream tasks.

Efficiency Comparison. In addition to performance evaluation, we also compare the training parameters of our method AdaRing, with existing VLM fine-tuning methods in the OxfordFlowers dataset. In Table 2, compared to MMA, AdaRing achieves a significant reduction in terms of training parameters by approximately 90%. Moreover, PromptKD relies on a computationally expensive two-stage process by first finetuning a large CLIP teacher model and then distilling the knowledge from the teacher model to the small student model. Besides, our AdaRing maintains a comparable parameter scale to that of CoOp and LASP while achieving significantly superior performance. These improved performances are induced by the compo-

nents of the cross-layer tensor ring decomposition and diverse adapters in AdaRing, which will be proved in the ablation studies.

6.2. Ablation Studies

Ablation of Main Components. To investigate the importance of cross-layer tensor ring decomposition (TRD) and the collaboration of diverse adapters, we conduct ablation studies on 3 datasets: FGVCAircraft, OxfordPets, and Food101 in Table 3, and present the results of MMA in row 1 as baseline. By comparing row 2 to row 1, AdaRing achieves a substantial reduction in parameter count by nearly 68% without sacrificing performance, demonstrating the effectiveness of our cross-layer TRD design. Additionally, built upon the cross-layer TRD design, our

Table 2. Efficiency comparison in terms of learnable parameters.

Method	CoOp	MaPLE	LASP	PromptKD	BSLoRA (SS)	BSLoRA (GT)	MMA	AdaRing
#Param. (M)	0.04	3.55	0.06	1.01	0.15	0.21	0.67	0.06

Table 3. Ablation study on the main components of AdaRing.

Method	Cross Layer	Diverse Adapter	# Param. (M)	FGVCAircraft		OxfordPets		Food101	
				Base	Novel	Base	Novel	Base	Novel
AdaRing	✗	✗	0.67	40.57	36.33	95.40	98.07	90.13	91.30
	✓	✗	0.29	42.83	36.77	95.45	98.00	90.24	91.10
	✓	✓	0.06	49.37	41.98	96.46	98.31	93.53	94.02

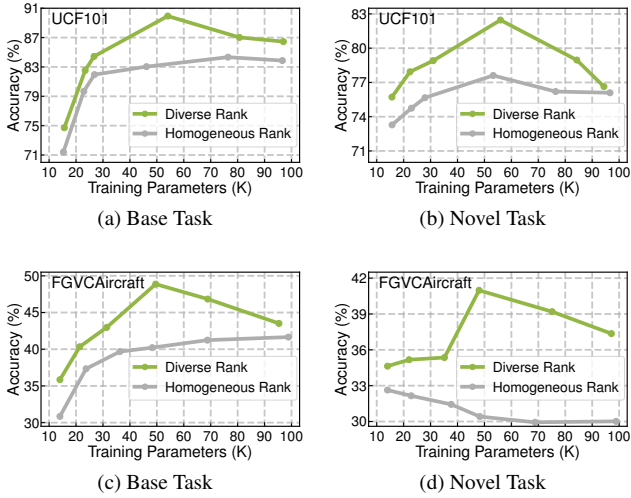


Figure 7. Impact of adapter diversity on performance under varying trainable parameter budgets.

diverse adapter design achieves better performance with fewer training parameters compared to its homogeneous counterpart (row 3 vs. row 2), demonstrating its efficiency in handling diverse tasks.

Diversity of Adapters. To further rigorously examine the impact of diversity in the adapter structure, we compare our diverse adapter design with the homogeneous adapter strategy within a certain range of parameters, by evaluating their performance on the base and novel tasks of UCF101 and FGVCAircraft datasets. As Figure 7 shown, with the increase of training parameters, the accuracy rises to a peak and then decreases for the base and novel tasks. More importantly, the model with diverse adapters consistently outperforms one with homogeneous adapters under the same number of training parameters. Specifically, we set the layer rank to 64 in the fine-grained adapter and the layer rank to 1 in the coarse-grained adapter.

Hyperparameters Analysis. Preservation ratio λ is a parameter controlling the balance of classification loss and generalization-aware regularization term during fine-

tuning. To determine the appropriate setting, we explore the influence of λ on model performance in the EuroSAT. Figure 8 shows that the accuracy on the novel task rises with the increase of λ . This rise can be attributed to the augmented generalization capacity of the model. However, we can observe that performances begin to decrease when the preservation ratio is larger than 0.5. This is because increasing the weight of the generalization-aware regularization term reduces the emphasis on the classification loss during training. Therefore, to achieve an optimal balance between classification accuracy and generalization regularization, we set $\lambda = 0.5$.

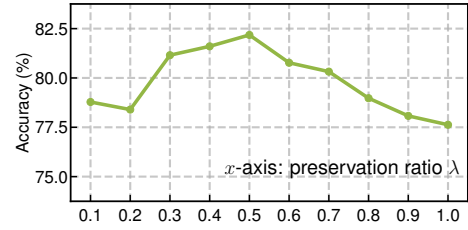


Figure 8. Influence of different preservation ratios on performance of novel task.

7. Conclusion

In this work, we propose a novel fine-tuning framework for extremely parameter-efficient vision & language model adaptation. Our approach AdaRing constructs the ultra-light adapter into layer-shared and layer-specific components based on the cross-layer tensor ring decomposition algorithm, addressing the high redundancy among layer-wise adapters. Moreover, the collaboration of adapters with varied granularity is developed to handle tasks that require distinct representational capacities. Finally, the diverse adapters are further encouraged to cooperate during the generalization-aware fine-tuning. Experiments on various downstream tasks demonstrate the superiority of our proposed AdaRing.

References

- [1] Lukas Bossard, Matthieu Guillaumin, and Luc Van Gool. Food-101—mining discriminative components with random forests. In *Computer vision—ECCV 2014: 13th European conference, zurich, Switzerland, September 6–12, 2014, proceedings, part VI 13*, pages 446–461, 2014. 6
- [2] Adrian Bulat and Georgios Tzimiropoulos. Lasp: Text-to-text optimization for language-aware soft prompting of vision & language models. In *Proceedings of the IEEE/CVF conference on computer vision and pattern recognition*, pages 23232–23241, 2023. 4, 6
- [3] Shoufa Chen, Chongjian Ge, Zhan Tong, Jiangliu Wang, Yibing Song, Jue Wang, and Ping Luo. Adaptformer: Adapting vision transformers for scalable visual recognition. *Advances in Neural Information Processing Systems*, 35:16664–16678, 2022. 1
- [4] Tianran Chen, Jiarui Chen, Baoquan Zhang, Zhehao Yu, Shidong Chen, Rui Ye, Xutao Li, and Yunming Ye. Sensitivity-aware efficient fine-tuning via compact dynamic-rank adaptation. In *Proceedings of the Computer Vision and Pattern Recognition Conference*, pages 9655–9664, 2025. 2
- [5] Seokju Cho, Heeseong Shin, Sunghwan Hong, Anurag Arnab, Paul Hongsuck Seo, and Seungryong Kim. Catseg: Cost aggregation for open-vocabulary semantic segmentation. In *Proceedings of the IEEE/CVF Conference on Computer Vision and Pattern Recognition*, pages 4113–4123, 2024. 1
- [6] Mircea Cimpoi, Subhransu Maji, Iasonas Kokkinos, Sammy Mohamed, and Andrea Vedaldi. Describing textures in the wild. In *Proceedings of the IEEE conference on computer vision and pattern recognition*, pages 3606–3613, 2014. 6
- [7] Jia Deng, Wei Dong, Richard Socher, Li-Jia Li, Kai Li, and Li Fei-Fei. Imagenet: A large-scale hierarchical image database. In *2009 IEEE conference on computer vision and pattern recognition*, pages 248–255, 2009. 6
- [8] Reza Esfandiarpour, Cristina Menghini, and Stephen Bach. If CLIP could talk: Understanding vision-language model representations through their preferred concept descriptions. In *Proceedings of the 2024 Conference on Empirical Methods in Natural Language Processing*, pages 9797–9819, Miami, Florida, USA, 2024. 3
- [9] Li Fei-Fei, Rob Fergus, and Pietro Perona. Learning generative visual models from few training examples: An incremental bayesian approach tested on 101 object categories. In *2004 conference on computer vision and pattern recognition workshop*, pages 178–178, 2004. 6
- [10] Peng Gao, Shijie Geng, Renrui Zhang, Teli Ma, Rongyao Fang, Yongfeng Zhang, Hongsheng Li, and Yu Qiao. Clip-adapter: Better vision-language models with feature adapters. *International Journal of Computer Vision*, 132(2): 581–595, 2024. 1, 2
- [11] Richard A Harshman et al. Foundations of the parafac procedure: Models and conditions for an “explanatory” multi-modal factor analysis. *UCLA working papers in phonetics*, 16(1):84, 1970. 3
- [12] Soufiane Hayou, Nikhil Ghosh, and Bin Yu. Lora+: Efficient low rank adaptation of large models. *arXiv preprint arXiv:2402.12354*, 2024. 3
- [13] Junxian He, Chunting Zhou, Xuezhe Ma, Taylor Berg-Kirkpatrick, and Graham Neubig. Towards a unified view of parameter-efficient transfer learning. In *International Conference on Learning Representations*, 2022. 3
- [14] Patrick Helber, Benjamin Bischke, Andreas Dengel, and Damian Borth. Eurosat: A novel dataset and deep learning benchmark for land use and land cover classification. *IEEE Journal of Selected Topics in Applied Earth Observations and Remote Sensing*, 12(7):2217–2226, 2019. 6
- [15] Edward J Hu, Yelong Shen, Phillip Wallis, Zeyuan Allen-Zhu, Yuanzhi Li, Shean Wang, Lu Wang, Weizhu Chen, et al. Lora: Low-rank adaptation of large language models. *ICLR*, 1(2):3, 2022. 1, 3
- [16] Max Jaderberg, Andrea Vedaldi, and Andrew Zisserman. Speeding up convolutional neural networks with low rank expansions. *arXiv preprint arXiv:1405.3866*, 2014. 3
- [17] Chao Jia, Yinfei Yang, Ye Xia, Yi-Ting Chen, Zarana Parekh, Hieu Pham, Quoc Le, Yun-Hsuan Sung, Zhen Li, and Tom Duerig. Scaling up visual and vision-language representation learning with noisy text supervision. In *International conference on machine learning*, pages 4904–4916, 2021. 1, 2, 3
- [18] Pengkun Jiao, Bin Zhu, Jingjing Chen, Chong-Wah Ngo, and Yu-Gang Jiang. Visual cue enhancement and dual low-rank adaptation for efficient visual instruction fine-tuning. *arXiv preprint arXiv:2411.12787*, 2024. 1
- [19] Can Jin, Ying Li, Mingyu Zhao, Shiyu Zhao, Zhenting Wang, Xiaoxiao He, Ligong Han, Tong Che, and Dimitris N Metaxas. Lor-vp: Low-rank visual prompting for efficient vision model adaptation. *arXiv preprint arXiv:2502.00896*, 2025. 1
- [20] Muhammad Uzair Khattak, Hanoona Rasheed, Muhammad Maaz, Salman Khan, and Fahad Shahbaz Khan. Maple: Multi-modal prompt learning. In *Proceedings of the IEEE/CVF conference on computer vision and pattern recognition*, pages 19113–19122, 2023. 6
- [21] Jonathan Krause, Michael Stark, Jia Deng, and Li Fei-Fei. 3d object representations for fine-grained categorization. In *Proceedings of the IEEE international conference on computer vision workshops*, pages 554–561, 2013. 6
- [22] Dongjun Lee, Seokwon Song, Jihee Suh, Joonmyeong Choi, Sanghyeok Lee, and Hyunwoo J Kim. Read-only prompt optimization for vision-language few-shot learning. In *Proceedings of the IEEE/CVF international conference on computer vision*, pages 1401–1411, 2023. 6
- [23] Zheng Li, Xiang Li, Xinyi Fu, Xin Zhang, Weiqiang Wang, Shuo Chen, and Jian Yang. Promptkd: Unsupervised prompt distillation for vision-language models. In *Proceedings of the IEEE/CVF Conference on Computer Vision and Pattern Recognition*, pages 26617–26626, 2024. 2, 6
- [24] Siqi Luo, Haoran Yang, Yi Xin, Mingyang Yi, Guangyang Wu, Guangtao Zhai, and Xiaohong Liu. Tr-pts: Task-relevant parameter and token selection for efficient tuning. *arXiv preprint arXiv:2507.22872*, 2025. 2

- [25] Subhansu Maji, Esa Rahtu, Juho Kannala, Matthew Blaschko, and Andrea Vedaldi. Fine-grained visual classification of aircraft. *arXiv preprint arXiv:1306.5151*, 2013. 6
- [26] Maria-Elena Nilsback and Andrew Zisserman. Automated flower classification over a large number of classes. In *2008 Sixth Indian conference on computer vision, graphics & image processing*, pages 722–729, 2008. 6
- [27] Omkar M Parkhi, Andrea Vedaldi, Andrew Zisserman, and CV Jawahar. Cats and dogs. In *2012 IEEE conference on computer vision and pattern recognition*, pages 3498–3505, 2012. 4, 6
- [28] Zelin Peng, Zhengqin Xu, Zhilin Zeng, Yaoming Wang, Lingxi Xie, Qi Tian, and Wei Shen. Parameter-efficient fine-tuning in hyperspherical space for open-vocabulary semantic segmentation. *arXiv preprint arXiv:2405.18840*, 2024. 1
- [29] David Pujol-Perich, Sergio Escalera, and Albert Clap  s. Sparse-dense side-tuner for efficient video temporal grounding. *arXiv preprint arXiv:2507.07744*, 2025. 2
- [30] Alec Radford, Jong Wook Kim, Chris Hallacy, Aditya Ramesh, Gabriel Goh, Sandhini Agarwal, Girish Sastry, Amanda Askell, Pamela Mishkin, Jack Clark, et al. Learning transferable visual models from natural language supervision. In *International conference on machine learning*, pages 8748–8763, 2021. 1, 6
- [31] Khurram Soomro, Amir Roshan Zamir, and Mubarak Shah. Ucf101: A dataset of 101 human actions classes from videos in the wild. *arXiv preprint arXiv:1212.0402*, 2012. 6
- [32] Ledyard R Tucker. Implications of factor analysis of three-way matrices for measurement of change. *Problems in measuring change*, 15(122-137):3, 1963. 3
- [33] An Wang, Xingwu Sun, Ruobing Xie, Shuaipeng Li, Jiaqi Zhu, Zhen Yang, Pinxue Zhao, JN Han, Zhanhui Kang, Di Wang, et al. Hmoe: Heterogeneous mixture of experts for language modeling. *arXiv preprint arXiv:2408.10681*, 2024. 2
- [34] Benyou Wang, Yuxin Ren, Lifeng Shang, Xin Jiang, and Qun Liu. Exploring extreme parameter compression for pre-trained language models. In *International Conference on Learning Representations*, 2022. 3
- [35] Rujie Wu, Xiaojian Ma, Hai Ci, Yue Fan, Yuxuan Wang, Haozhe Zhao, Qing Li, and Yizhou Wang. Longvitu: Instruction tuning for long-form video understanding, 2025. 1
- [36] Jianxiong Xiao, James Hays, Krista A Ehinger, Aude Oliva, and Antonio Torralba. Sun database: Large-scale scene recognition from abbey to zoo. In *2010 IEEE computer society conference on computer vision and pattern recognition*, pages 3485–3492, 2010. 6
- [37] Jinqi Xiao, Miao Yin, Yu Gong, Xiao Zang, Jian Ren, and Bo Yuan. Comcat: towards efficient compression and customization of attention-based vision models. *arXiv preprint arXiv:2305.17235*, 2023. 2
- [38] Jinqi Xiao, Chengming Zhang, Yu Gong, Miao Yin, Yang Sui, Lizhi Xiang, Dingwen Tao, and Bo Yuan. Haloc: hardware-aware automatic low-rank compression for compact neural networks. In *Proceedings of the AAAI Conference on Artificial Intelligence*, pages 10464–10472, 2023. 2
- [39] Kun Xie, Can Liu, Xin Wang, Xiaocan Li, Gaogang Xie, Jigang Wen, and Kenli Li. Neural network compression based on tensor ring decomposition. *IEEE Transactions on Neural Networks and Learning Systems*, 36(3):5388–5402, 2024. 4
- [40] Lingxiao Yang, Ru-Yuan Zhang, Yanchen Wang, and Xiaohua Xie. Mma: Multi-modal adapter for vision-language models. In *Proceedings of the IEEE/CVF Conference on Computer Vision and Pattern Recognition*, pages 23826–23837, 2024. 1, 2, 6
- [41] Yifan Yang, Kai Zhen, Ershad Banijamal, Athanasios Mouchtaris, and Zheng Zhang. Adazeta: Adaptive zeroth-order tensor-train adaption for memory-efficient large language models fine-tuning. *arXiv preprint arXiv:2406.18060*, 2024. 3, 4
- [42] Yifan Yang, Jiajun Zhou, Ngai Wong, and Zheng Zhang. Loretta: Low-rank economic tensor-train adaptation for ultra-low-parameter fine-tuning of large language models. In *Proceedings of the 2024 Conference of the North American Chapter of the Association for Computational Linguistics: Human Language Technologies*, pages 3161–3176, 2024. 3, 5
- [43] Hantao Yao, Rui Zhang, and Changsheng Xu. Visual-language prompt tuning with knowledge-guided context optimization. In *Proceedings of the IEEE/CVF conference on computer vision and pattern recognition*, pages 6757–6767, 2023. 2, 6
- [44] Miao Yin, Yang Sui, Wanzhao Yang, Xiao Zang, Yu Gong, and Bo Yuan. Hodec: Towards efficient high-order decomposed convolutional neural networks. In *Proceedings of the IEEE/CVF Conference on Computer Vision and Pattern Recognition*, pages 12299–12308, 2022. 2
- [45] Jiazuo Yu, Yunzhi Zhuge, Lu Zhang, Ping Hu, Dong Wang, Huchuan Lu, and You He. Boosting continual learning of vision-language models via mixture-of-experts adapters. In *Proceedings of the IEEE/CVF Conference on Computer Vision and Pattern Recognition*, pages 23219–23230, 2024. 1, 2
- [46] Qibin Zhao, Guoxu Zhou, Shengli Xie, Liqing Zhang, and Andrzej Cichocki. Tensor ring decomposition. *arXiv preprint arXiv:1606.05535*, 2016. 2, 3, 4
- [47] Wangbo Zhao, Jiasheng Tang, Yizeng Han, Yibing Song, Kai Wang, Gao Huang, Fan Wang, and Yang You. Dynamic tuning towards parameter and inference efficiency for vit adaptation. *arXiv preprint arXiv:2403.11808*, 2024. 1, 2
- [48] Kaiyang Zhou, Jingkang Yang, Chen Change Loy, and Ziwei Liu. Conditional prompt learning for vision-language models. In *Proceedings of the IEEE/CVF conference on computer vision and pattern recognition*. 1, 2, 4
- [49] Kaiyang Zhou, Jingkang Yang, Chen Change Loy, and Ziwei Liu. Learning to prompt for vision-language models. *International Journal of Computer Vision*, 130(9):2337–2348, 2022. 1, 2, 6
- [50] Yuhua Zhou, Ruifeng Li, Changhai Zhou, Fei Yang, and Aimin PAN. BSLoRA: Enhancing the parameter efficiency of loRA with intra-layer and inter-layer sharing. In *Forty-second International Conference on Machine Learning*, 2025. 6